ISSN 0021-3640, JETP Letters, 2016, Vol. 104, No. 2, pp. 88–93. © Pleiades Publishing, Inc., 2016.
Original Russian Text © A.M. Balagurov, I.A. Bobrikov, S.V. Sumnikov, V.Yu. Yushankhai, N. Mironova-Ulmane, 2016, published in Pis'ma v Zhurnal Eksperimental'noi i Teoreticheskoi Fiziki, 2016, Vol. 104, No. 2, pp. 84–90.

CONDENSED MATTER

Magnetostructural Phase Transitions in NiO and MnO: Neutron Diffraction Data

A. M. Balagurov[a],*, I. A. Bobrikov[a], S. V. Sumnikov[a], V. Yu. Yushankhai[a], and N. Mironova-Ulmane[b]

[a] *Joint Institute for Nuclear Research, Dubna, Moscow region, 141980 Russia*

[b] *Institute of Solid State Physics, University of Latvia, LV-1063 Riga, Latvia*

**e-mail: bala@nf.jinr.ru*

Received April 12, 2016; in final form, May 30, 2016

Structural and magnetic phase transitions in NiO and MnO antiferromagnets have been studied by high-precision neutron diffraction. The experiments have been performed on a high-resolution Fourier diffractometer (pulsed reactor IBR-2), which has the record resolution for the interplanar distance and a high intensity in the region of large interplanar distances; as a result, the characteristics of both transitions have been determined simultaneously. It has been shown that the structural and magnetic transitions in MnO occur synchronously and their temperatures coincide within the experimental errors: $T_{str} \approx T_{mag} \approx (119 \pm 1)$ K. The measurements for NiO have been performed with powders with different average sizes of crystallites (~1500 nm and ~138 nm). It has been found that the transition temperatures differ by ~50 K: $T_{str} = (471 \pm 3)$ K, $T_{mag} = (523 \pm 2)$ K. It has been argued that a unified mechanism of the "unsplit" magnetic and structural phase transition at a temperature of T_{mag} is implemented in MnO and NiO. Deviation from this scenario in the behavior of NiO is explained by the quantitative difference—a weak coupling between the magnetic and secondary structural order parameters.

DOI: 10.1134/S0021364016140071

1. INTRODUCTION

An interest in the investigation of physical and physicochemical properties of antiferromagnetic monoxides of transition metals (MnO, NiO, FeO, and CoO) has been supported for several decades because of the importance of this class of materials for theoretical models of magnetism and for their numerous applications. General information on the magnetic and structural phase transitions in simple oxides was obtained in the middle of the past century. The hypothesis of the existence of antiferromagnetic ordering in crystals was confirmed for the first time in the neutron diffraction study of MnO [1]. In the same years, it was established [2, 3] that a small structural distortion reducing the initial cubic symmetry appears in these oxides below the Néel temperature T_N. In MnO, NiO, and FeO, it is reduced to the rhombohedral symmetry; i.e., compression or extension occurs along one of the [111] directions of the cube. The magnetic structure of all four mentioned oxides was studied in detail in [4] by the neutron diffraction method; in particular, it was established that, for MnO and NiO at a low temperature of 4.2 K, the magnetic moments of Mn and Ni are ferromagnetically ordered in (111) planes, which in turn are antiferromagnetically ordered along one of the [111] crystallographic directions.

Already in the early stage of subsequent investigations, the spin J_1–J_2 model justifying the main features of magnetically ordered structures in these systems was formulated [5]. According to the general principles of the theory of superexchange [6], for ions of $3d$ metals localized at sites of the initial fcc lattice, the isotropic antiferromagnetic exchange J_2 (>0) between the second neighbors usually dominates ($J_2 > |J_1|$) over a weaker (antiferromagnetic or ferromagnetic) exchange J_1 between the nearest neighbors. The effects of magnetocrystalline anisotropy with the characteristic energy $\sim K$ and the corresponding orbital contribution to the observed magnetic moments caused by the spin–orbit interaction in the $3d$ electron shell of magnetic ions provide a noticeable influence ($K \sim 1$ meV) for monoxides with Jahn–Teller ions, Co^{2+} and Fe^{2+}, but are absent for Mn^{2+} ($K = 0$) and are extremely weak for Ni^{2+} ($K \sim 10^{-2}$ meV) [7]. Such a behavior is explained by the almost complete "freezing" of the orbital angular momentum of Mn^{2+} and Ni^{2+} ions, so that the magnetic anisotropy in MnO and NiO is due predominantly to a weak dipole interaction between magnetic moments.

The last circumstance, as well as the estimates of the isotropic exchange, $J_1 \approx -1.4$ meV, $J_2 \approx 19$ meV

for NiO [8, 9] and $J_1 \approx 0.37$ meV, $J_2 \approx 0.45$ meV for MnO [10, 11], indicates that the antiferromagnetic transition in these compounds can occur within a unified exchange-striction mechanism. According to this mechanism, which implies the dependence of exchange interactions on interatomic distances and was studied in a number of early works [12, 13], the stabilization of the free magnetic energy and the magnetic ordering at the point T_N with a decrease in the temperature are accompanied by a simultaneous structural transition. An additional argument in favor of the scenario with the "unsplit" magnetostructural transition follows from the geometric frustration of the exchange J_1–J_2 interaction on the fcc lattice [14, 15]. Indeed, the dominant antiferromagnetic exchange J_2 tends to establish the Néel order in each of four simple cubic sublattices, but the directions of the magnetization of sublattices are independent at any sign of the exchange J_1. Such a continual degeneracy can be lifted and a long-range magnetic order with the united antiferromagnetism vector throughout the entire crystal can be established because of the breaking of symmetry through the structural lattice deformation or because of the "order-from-disorder" mechanism [16]. In the latter case, the breaking of the symmetry of the lattice at the magnetic transition point is not required and (in the presence of independent structural instability of the lattice) the structural transition can be observed at temperatures below T_N.

Using the methods of density functional theory, the authors of [7] calculated the possible structural distortions accompanying the formation of the long-range antiferromagnetic order in MnO, NiO, FeO, and CoO and listed all references existing at that time to experimental data on the characteristics of structural and magnetic phase transitions in these oxides. The situation for MnO seems completely clear because there are detailed reliable data on the temperature dependences of the rhombohedral distortion angle α_R and the ordered magnetic moment M. In particular, according to the experimental data obtained in [17] (see also references therein) for MnO by the neutron diffraction method, the temperatures of both transitions, T_{str} and T_{mag}, in this oxide coincide with each other within ~0.5 K.

The above brief analysis indicates closeness of the magnetic interactions in MnO and NiO, and a qualitatively unified scenario of the "unsplit" magnetostructural transition for them can be proposed. However, a clear conclusion cannot be made on the basis of the existing experimental data for NiO. X-ray diffraction studies that we know were focused on the rhombohedral distortion value, whereas the structural transition temperature was determined only approximately and the values obtained were close to 480 K (see, e.g., [18, 19]). Analyzing the polarization microscopy results for the NiO single crystal, Springthorpe [20] concluded that T_{str} and T_{mag} are the same. A similar conclusion was made in [21], where the transition temperatures were determined from the measurements of the magnetic susceptibility, $T_{mag} = (516 \pm 2)$ K, and X-ray topography, $T_{str} = (517 \pm 3)$ K. The most accurate value $T_{mag} = 524.5$ K for NiO was apparently obtained in [22] in the measurements of the magnetic susceptibility. At the same time, the values $T_{mag} = 528.8$ and 530 K were obtained in neutron diffraction experiments with various data processing data [23].

The analysis of the structural and magnetic phase transitions in simple antiferromagnetic oxides in terms of neutron diffraction has an important advantage over other methods. Indeed, since nuclear and magnetic peaks do not overlap in measured neutron diffraction patterns, the characteristics of both transitions can be determined independently in the same measurement and, correspondingly, on the same sample. However, in the case of NiO, the comparison of structural and magnetic transition temperatures is complicated because the distortion of the cubic symmetry in this oxide is very small: according to X-ray data, the difference of the rhombohedral angle from 60° at $T = 5$ K is as small as 0.09°, which is one-eighth of that in MnO. Correspondingly, the characteristics of the structural and magnetic transitions cannot be measured simultaneously on a neutron diffractometer that is optimized for the analysis of magnetic structures and has not very high resolution. For this reason, a small rhombohedral distortion of the lattice of NiO was ignored in [23]. Necessary conditions for such an experiment are high resolution, sufficient for the magnetic moment of small structural distortions, and a high luminosity in the region of large interplanar distances, where comparatively weak magnetic diffraction peaks are located. A high-resolution Fourier diffractometer (HRFD) operating at the IBR-2 pulsed reactor (Joint Institute for Nuclear Research, Dubna) satisfies these conditions. Results obtained on this diffractometer for NiO and MnO are reported in this work. We measured the temperature dependences of the characteristics of the structural and magnetic phase transitions in them (for the first time for NiO) and showed that the difference between the transition temperatures for MnO is no more than 2 K, whereas this difference for NiO reaches ~50 K.

2. EXPERIMENT

Nickel oxide samples were fabricated at the Institute of Solid State Physics, University of Latvia (Riga), from commercially available (99.9%) NiO powder. First, light green nanopowder (below, NiO-1) with a specific surface of 6.4 m^2/g and with average sizes of crystallites of about 138 nm according to the BET method was obtained by the technology

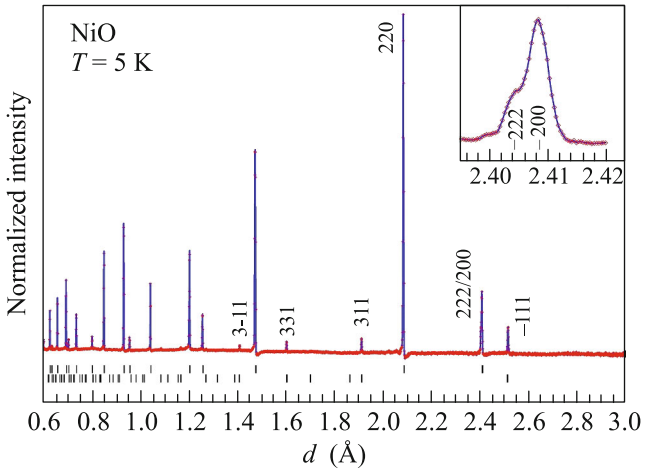

Fig. 1. (Color online) Neutron diffraction spectrum of NiO measured with the HRFD at a low temperature in the high-resolution mode. The upper and lower series of vertical dashes mark the positions of the crystal and magnetic diffraction peaks, respectively. The Miller indices (for the large R lattice) are present for several magnetic and first crystal diffraction peaks. The inset shows the splitting of the (200) and (222) peaks because of rhombohedral distortion. The relative splitting value is about 0.0018. A slightly asymmetric shape of peaks with a dip on the right is due to the features of the correlation method of data recording on the HRFD.

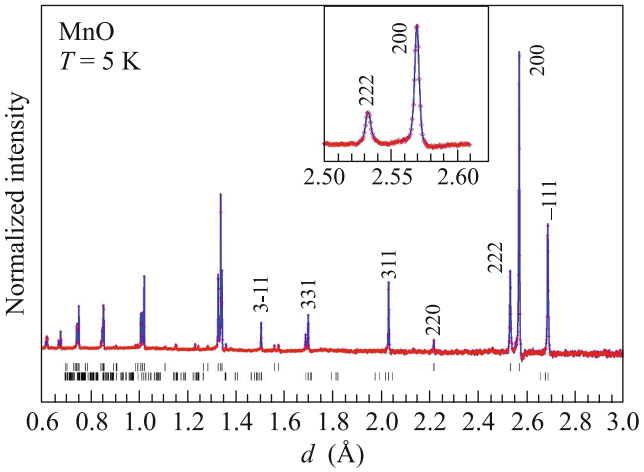

Fig. 2. (Color online) Neutron diffraction spectrum of MnO measured with the HRFD at a low temperature in the high-resolution mode. The upper and lower series of vertical dashes mark the positions of the crystal and magnetic diffraction peaks, respectively. The Miller indices (for the large R lattice) are present for several magnetic and first crystal diffraction peaks. The inset shows the splitting of the (200) and (222) peaks because of rhombohedral distortion. The relative splitting value is about 0.0144.

described in [24]. Then, a part of this powder was annealed at 1000°C; as a result, its specific surface decreased to 0.6 m^2/g and the average sizes of crystallites were 1500 nm (according to BET data). This powder (below, NiO-2) had dark green color, indicating the absence of a noticeable amount of stacking faults. Commercially available X-ray pure MnO powder (REAKhIM, TU 6-09-3217-78) was used as manganese oxide.

Neutron diffraction spectra were measured with the HRFD [25] at the IBR-2 pulsed reactor. The HRFD is a correlation spectrometer in time of flight (TOF diffractometer) whose resolution in the interplanar distance is determined by the maximum rate of a fast Fourier chopper. In the standard operation mode (V_{max} = 4000 rpm), $\Delta d/d \approx 0.001$ at d = 2 Å and the resolution depends slightly on d_{hkl}, slightly improving at large d_{hkl} values. Simultaneously with the recording of "high-resolution" diffraction spectra, the HRFD records standard (without the correlation analysis) TOF spectra with an "intermediate" resolution of $\Delta d/d \approx 0.01$–0.02. The design of the HRFD makes it possible to collect diffraction information with a high resolution by backscattering detectors ($2\theta = 152°$) in the range d_{hkl} = 0.6–3.6 Å and by a detector at $2\theta = 90°$ in the range d_{hkl} = 0.8–4.9 Å. In the intermediate-resolution mode, the same detectors record spectra in the ranges to 4.5 and 6.0 Å, respectively. The quality of diffraction spectra measured on all three samples is good and no impurity phases were revealed. Measurements with nickel oxides were performed at an increase in the temperature from room temperature to 543 K and individually at T = 5 K. Manganese oxide was measured at an increase in the temperature from 5 to 130 K.

The atomic symmetry of both oxides in the paramagnetic phase is cubic (space group $Fm\bar{3}m$, $a_{NiO} \approx 4.175$ Å, $a_{MnO} \approx 4.448$ Å). Below the Néel temperature T_N, rhombohedral distortion appears (space group $R\bar{3}m$) and the rhombohedral angle at T = 5 K differs from 60° by $\Delta\alpha_R = 0.09(1)°$ for NiO and by $\Delta\alpha_R = 0.72(1)°$ for MnO. Below T_N, the magnetic moments of Ni are ordered antiferromagnetically with the translation vector k = [1/2 1/2 1/2] in a cubic cell. The rhombohedral magnetic cell is doubled in linear parameters as compared to the atomic cell, whereas the rhombohedral angle does not change. Below, the Miller indices of all (nuclear and magnetic) neutron diffraction peaks are presented in the magnetic cell called the large R cell.

The neutron diffraction spectra from NiO-2 and MnO measured at a low temperature of 5 K are shown in Figs. 1 and 2, respectively. Large differences between them are caused by two reasons: the coherent scattering lengths of Ni and Mn differ not only in magnitude but also in sign ($b_{Ni} = 1.030$ and $b_{Mn} = -0.373$ in units of 10^{-12} cm) and the difference between the rhombohedral distortions is large. The maximum interplanar distance in the large R cell of NiO is

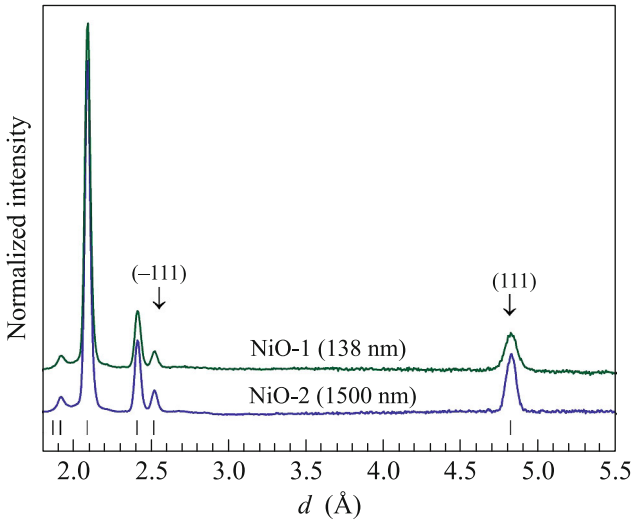

Fig. 3. (Color online) Segments of the spectra measured at room temperature in the intermediate-resolution mode in the region of large d_{hkl} values for nickel oxide samples. The vertical dashes mark the positions of peaks in the magnetic cell and the Miller indices are indicated for the first two antiferromagnetic peaks.

4.82 Å. The corresponding (111) magnetic peak is clearly observed in neutron diffraction spectra measured in the intermediate resolution mode (Fig. 3).

3. PROCESSING OF EXPERIMENTAL DATA

Diffraction data were analyzed by the Rietveld method with the MRIA [27] and FullProf [28] software packages involving built-in tables for coherent scattering lengths and magnetic form factors. The unit cell parameters, the thermal factor of oxygen, and the magnitude of the magnetic moment were refined. The quantities χ^2 and R_ω varying about 2 and 5%, respectively, indicate a high quality of processing. For illustration, one of the Rietveld-processed spectra is shown in Fig. 4.

The temperature dependences of the deviation of the rhombohedral angle from 60° and the magnetic moment were approximated by the empirical formula $F(T) \sim (1-(T/T_c)^q)^\beta$, which usually makes it possible to cover the entire temperature scale. At temperatures close to T_c, this formula is modified to the standard expression $F(T) \sim (1-T/T_c)^\beta$, where the critical exponent β is 0.326 or 0.367 for the 3D Ising or Heisenberg model of magnetism, respectively. The dependences obtained for the rhombohedral distortion angle $\Delta\alpha_R = \alpha_R - 60°$ and for the magnetic moment of the metal atom are shown in Fig. 5 (for MnO) and Fig. 6 (for NiO), and the numerical data are summarized in the table.

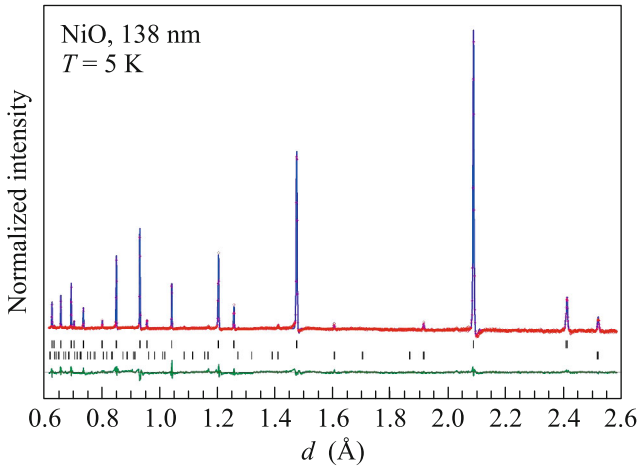

Fig. 4. (Color online) Spectrum of the NiO-1 (138 nm) sample measured at 5 K processed by the Rietveld method. Shown are the experimental points, calculated function, and (lower) difference curve normalized to the error at point. The upper and lower series of vertical dashes mark the positions of the crystal and magnetic diffraction peaks, respectively.

4. DISCUSSION AND CONCLUSIONS

The main conclusion following from the reported results is that the difference between the temperatures of the structural and magnetic transitions for MnO is within the experimental errors ($T_{str} \approx T_{mag}$), whereas this difference for both NiO samples is far beyond the possible errors. Indeed, the averaging of the transition temperatures for NiO-1 and NiO-2 gives $T_{str} = (471 \pm 3)$ K and $T_{mag} = (523 \pm 2)$ K; i.e., $\Delta T \approx 50$ K.

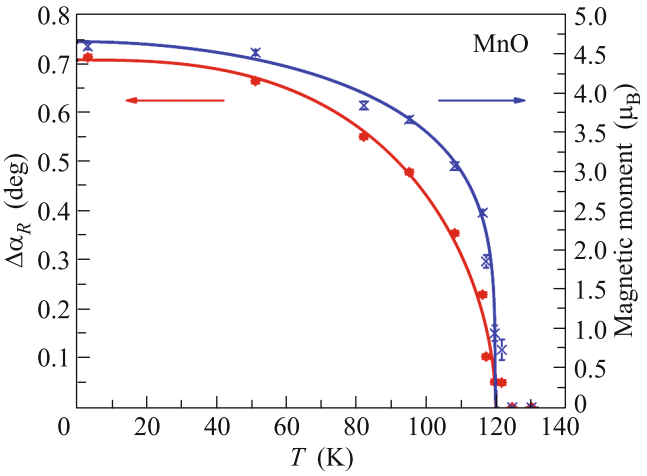

Fig. 5. (Color online) Temperature dependence of the rhombohedral distortion angle (left scale, red points) and magnetic moment (right scale, blue points) for MnO. Experimental errors are close to the sizes of points.

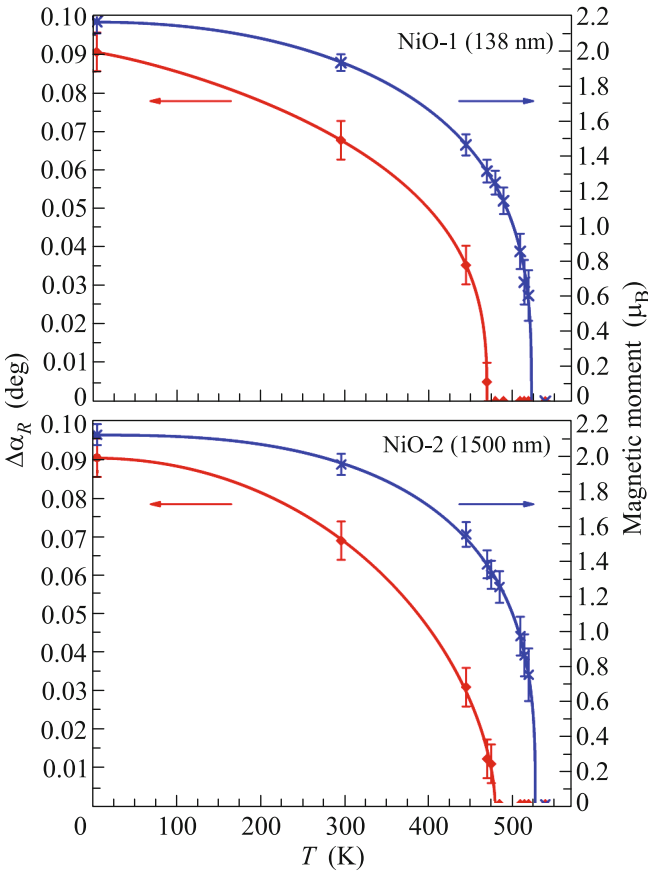

Fig. 6. (Color online) Temperature dependence of the rhombohedral distortion angle (left scale, red points) and magnetic moment (right scale, blue points) for NiO-1 and NiO-2.

The results for MnO are in good agreement with reported data. In particular, according to the neutron diffraction data and plots reported in [18], $T_{mag} \approx 118.0$ K, $\Delta\alpha_C \approx 0.61°$, and $\beta_{mag} \approx 0.17$. Here, $\Delta\alpha_C$ is the rhombohedral distortion in the cubic cell related to $\Delta\alpha_R$ as $\Delta\alpha_C = \sqrt{3}/2\Delta\alpha_R$, wherefrom $\Delta\alpha_R = 0.70°$. Our temperature of the structural transition, T_{str}, for both NiO samples is close to the data reported in [18, 19] and explicitly contradicts the results presented in [20, 21]. The temperature of the magnetic transition, T_{mag}, coincides within the errors with the data for the magnetic susceptibility from [22] ($T_{mag} = 524.5$ K) and is slightly smaller than the values from [23] (528–530 K). At the same time, the critical exponent determined in [23] as $\beta_{mag} = 0.328 \pm 0.002$ is in agreement with the value presented in the table. The observed discrepancy in the data obtained by different methods and with different samples indicates that the characteristics of both transitions should be measured simultaneously and with the same sample, as was done in this work.

A physical mechanism explaining such a significant difference in the behavior of NiO and MnO is still unknown. A similar situation was observed in [17]. Indeed, the neutron diffraction experiments in $Fe_{0.92}O$ exhibit two transitions with largely different temperatures: the magnetic transition at $T_{mag} \approx 202$ K and the structural transition at $T_{str} \approx 160$ K. However, such a behavior in nonstoichiometric compounds $Fe_{1-x}O$ at $x \sim (0.01–0.1)$ was attributed in [28] to the effect of defects. The authors of [29, 30] give a critical review and a comparative analysis of numerous reported data on the magnetic and structural behaviors of MnO and $Fe_{1-x}O$ obtained in various experiments in a wide range of temperatures and external pressures. In the theoretical approach developed on this basis [28, 30] within the Landau phenomenological theory, a description of the magnetic and structural properties near the antiferromagnetic transition is proposed for the entire family of simple oxides MnO, NiO, FeO, and CoO with the unified functional for the free energy of the system. Simple oxides assumingly exhibit two types of instability, magnetic (with the order parameter m) at T_{mag} and structural (with the order parameter $q \sim \Delta\alpha$) at T_{str}, which are coupled to each other through the unified shear deformation of the lattice. This coupling is responsible for the linear–quadratic interaction $\lambda q m^2$ with the parameter λ whose magnitude is not universal for the entire family. A universal requirement following from the analysis of experimental data is that the magnetic transition dominates for all members of the family; i.e., $T_{mag} \geq T_{str}$, and the appearance of the antiferromagnetic order ($m \neq 0$) because of the interaction $\lambda q m^2$ is necessarily accompanied by the appearance of structural distortion ($q \neq 0$). Different regimes of the behavior m and q are possible depending on the parameters of the proposed model, in particular, on the closeness of T_{str} to T_{mag} and the coupling intensity, which is $\sim \lambda$. For example, if T_{str} is far from T_{mag} and coupling is weak, a continuous magnetic transition occurs and is accompanied below T_{mag} by a slight increase in the secondary order parameter according to $q \approx \gamma m^2$, where $\gamma \ll 1$. With a further decrease in T, as it approaches T_{str}, crossover in the temperature behavior of the structural distortion q appears at a certain temperature T^* ($T_{str} < T^* < T_{mag}$): the weak dependence of q mentioned above changes to a fast monotonic increase at the continuing regular growth of the magnetic order parameter m. Crossover is absent in the model regime with T_{str} close to T_{mag} and at strong coupling. In this limit, the magnetic transition at T_{mag}, which is accompanied by strong structural distortion $q \neq 0$, can acquire features of a weak first-order phase transition [29].

First three rows: the parameters of the crystal R cell and the magnetic moment of the cation obtained by processing diffraction spectra measured at $T = 5$ K. The next two triples of rows give the parameters (T, β, q) obtained from the approximation of the temperature dependences of the rhombohedral distortion angle and magnetic moment by the formula $F(T) = F_0(1 - (T/T_c)^q)^\beta$

Quantity	MnO	NiO-1	NiO-2
a, Å	3.1199(1)	2.9465(1)	2.9466(1)
α, deg	60.72(1)	60.09(1)	60.09(1)
M, μ_B	4.58(4)	2.16(7)	2.11(6)
T_{str}, K	119.8(8)	469(3)	478(5)
β_{str}	0.5(2)	0.34(5)	0.57(14)
q_{str}	2.8(1.1)	1.2(5)	2.0(6)
T_{mag}, K	119.6(5)	522(2)	526(3)
β_{mag}	0.23(4)	0.31(2)	0.33(3)
q_{mag}	1.9(8)	2.1(2)	2.7(3)

Within this model, the existence of two different scenarios of the magnetic and structural behaviors of simple antiferromagnetic oxides near the magnetic phase transition can explain contrasting behaviors of NiO and MnO, which were mentioned previously and have been confirmed by our observations. Indeed, a comparatively small distortion of the lattice in NiO ($\Delta\alpha = 0.09°$ at $T = 5$ K) indicates the weakness of the interaction and, as a result, the existence of the time interval $T^* < T < T_{mag} \approx 523$ K for this compound with a finite but very small unobservable value (taking into account the real accuracy of the measurements) of rhombohedral distortion. In this case, a rapid increase in $\Delta\alpha_R$ with a decrease in T below the crossover temperature, $T < T^*$, can be described by a monotonic dependence. Correspondingly, the formal description of the temperature behavior of $\Delta\alpha_R$ at $T < T^*$ by the monotonic dependence as in Fig. 6 can be erroneously treated as evidence of the independent structural transition at $T_{str} \approx 471$ K. An accurate magnetic moment of the rhombohedral distortion angle in NiO on a synchrotron radiation source in the temperature range $T_{str} - T_{mag}$ could provide additional reasons in favor of a certain model of the transition.

We are grateful to V.L. Aksenov and I.V. Golosovskii for stimulating discussions. This work was supported by the Russian Foundation for Basic Research (project no. 14-29-04091 ofi_m). The neutron experiments were performed with the IBR-2 neutron source (Joint Institute for Nuclear Research, Dubna).

REFERENCES

1. C. G. Shull and J. S. Smart, Phys. Rev. **76**, 1256 (1949).
2. H. P. Rooksby, Nature **152**, 304 (1943).
3. B. T. M. Willis and H. P. Rooksby, Acta Crystallogr. **6**, 827 (1953).
4. W. L. Roth, Phys. Rev. **110**, 1333 (1958).
5. D. Ter Haar and M. E. Lines, Phil. Trans. R. Soc. London A **254**, 521 (1962), Phil. Trans. R. Soc. London A **255**, 1 (1962).
6. P. W. Anderson, in *Solid State Physics: Advances in Research and Applications,* Vol. 14, Ed. by F. Seitz and D. Turnbull (Academic, New York, London, 1963).
7. A. Schrön, C. Rödl, and F. Bechstedt, Phys. Rev. B **86**, 115134 (2012).
8. M. Hutchings and E. Samuelsen, Phys. Rev. B **6**, 3447 (1972).
9. D. Köddeitzsch, W. Hergert, W. M. Temmerman, Z. Szotek, A. Ernst, and H. Winter, Phys. Rev. B **66**, 064434 (2002).
10. G. Pepy, J. Phys. Chem. Sol. **35**, 433 (1974).
11. I. Solovyev and K. Terakura, Phys. Rev. **58**, 15496 (1998).
12. M. E. Lines and E. D. Jones, Phys. Rev. A **139**, 1313 (1965).
13. M. E. Lines, Phys. Rep. **55**, 133 (1979).
14. T. Yildirim, A. B. Harris, and E. F. Shender, Phys. Rev. B **58**, 3144 (1998).
15. A. N. Ignatenko, A. A. Katanin, and V. Yu. Irkhin, JETP Lett. **87**, 555 (2008).
16. J. Villain, R. Bidaux, J.-P. Carton, and R. Conte, J. Phys. (France) **41**, 1263 (1980).
17. A. P. Kantor, L. S. Dubrovinsky, N. A. Dubrovinskaia, I. Yu. Kantor, and I. N. Goncharenko, J. Alloys Compd. **402**, 42 (2005).
18. H. P. Rooksby, Acta Crystallogr. **1**, 226 (1948).
19. L. C. Bartel and B. Morosin, Phys. Rev. B **3**, 1039 (1971).
20. A. J. Springthorpe, Phys. Status Solidi **24**, K3 (1967).
21. M. W. Vernon, Phys. Status Solidi **37**, K1 (1970).
22. G. Srinivasan and M. S. Seehra, Phys. Rev. B **29**, 6295 (1984).
23. T. Chatterji, G. J. McIntyre, and P.-A. Lindgard, Phys. Rev. B **79**, 172403 (2009).
24. N. Mironova-Ulmane, A. Kuzmin, I. Steins, J. Grabis, I. Sildos, and M. Pärs, J. Phys.: Conf. Ser. **93**, 172403 (2007).
25. A. M. Balagurov, Neutron News **16**, 8 (2005).
26. V. B. Zlokazov and V. V. Chernyshev, J. Appl. Crystallogr. **25**, 447 (1992).
27. J. Rodriguez-Carvajal, Physica B **192**, 55 (1993).
28. M. A. Carpenter, Z. Zhang, and Ch. J. Howard, J. Phys.: Condens. Matter **24**, 156002 (2012).
29. Z. Zhang, N. Church, S.-Ch. Lappe, M. Reinecker, A. Fuith, P. J. Saines, R. J. Harrison, W. Schranz, and M. A. Carpenter, J. Phys.: Condens. Matter **24**, 215404 (2012).
30. E. K. Salje and M. A. Carpenter, J. Phys.: Condens. Matter **23**, 462202 (2011).

Translated by R. Tyapaev